Observations of the vertical structure of a stratus cloud and radiation fogs in relation to the mechanism of drizzle formation

By T. OKITA, *The Department of Industrial Health and Hygiene, The Institute of Public Health, Tokyo, Japan*

(Manuscript received September 10, 1961)

ABSTRACT

Observations of the vertical structure of radiation fogs and a stratus cloud were made by means of a rotary droplet sampler and other techniques. The results of the surveys of four radiation fogs and one stratus cloud are presented. It is found that the upper part of a deep fog or a stratus cloud has a similar physical structure to a cumulus cloud. The observation reveals that ordinary fog droplets grow mainly by condensation. It is also found that the presence of large droplets of radii about 50 microns or more near the top of the fog or stratus cloud is a necessary condition for the production of drizzle. The rate of growth of the large droplets is approximately explained by the Langmuir's accretion theory.

Part I. Vertical structure of radiation fog and stratus cloud

1. Introduction

The physical properties of fog and stratus clouds, such as liquid water content, droplet concentration and droplet size, have been studied by many investigators. However, it is noted that the droplet measurements have been made almost entirely near the base of the fog or cloud and very few studies have been undertaken on their vertical structure.

The author devised a new sampler using water-blue dye-coated celluloid film for the measurement of the droplets in the upper part of fogs. The observations of radiation fog and a stratus cloud by means of this sampler and other gravity settling techniques revealed their vertical structure.

2. Structure of inland stratus cloud

On summer mornings stratus clouds are occasional phenomena over the inland area of Hokkaido, Japan; on the slope of the mountain they are observed as fogs.

In the early morning of August 10, 1959 a stratus cloud covered the Kamikawa Basin and the hills surrounding it. Droplet samplings were made across the cloud on the north-western slope of Mt. Tokachi (altitude 2070 m) by means of the gravity settling method (OKITA, 1961).

We started from Shirogane (altitude 650 m) at 0445 JST, when the cloud base was about 50 m above the ground. After making droplet samplings at several places along the road we arrived at Bogakudai (1200 m) at 0617 JST, where we found ourselves above the cloud top. There was an altostratus cloud deck completely covering the sky but no rain was observed falling from the cloud. We then made several samplings of cloud droplets while going down along the same road and when we returned finally to Shirogane at 0728 JST, the cloud base was still 50 m above Shirogane. White birch trees, 2–3 m high, were planted irregularly along the road near Shirogane, but above 750 m there was a wide area of bare ground or bush.

Figs. 1*a–f* represent the cross-sectional distributions of droplet concentrations and other factors in the stratus cloud. In the figures the numerals above and below the slope line are the values measured on the way upward and downward respectively.

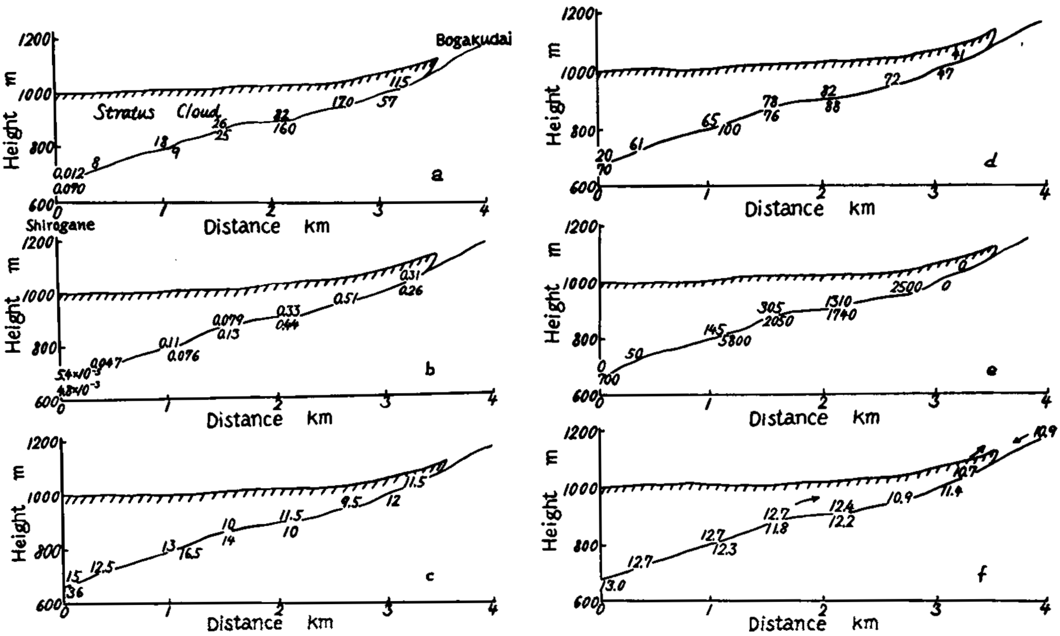

FIG. 1. (*a*) Droplet concentration cm^{-3}; (*b*) liquid water content g/m^3; (*c*) mean volume radius μ (*d*) Maximum droplet radius μ; (*e*) large droplet concentration $m^{-3} r \geqslant 50\ \mu$; (*f*) air temperature °C.

Figs. 1*a* and *c* show that in the upper part of the cloud droplets were relatively smaller and their concentration was above 100 cm^{-3}, while in the lower part they were fewer and larger. The liquid water content of the cloud was usually greater than 0.3 g/m^3 in the upper part of the cloud, while in the lower part it was less than 0.1 g/m^3. The maximum values of the size and concentration of large droplets were found in the middle part of the cloud. It is of interest to note that the large cloud droplets with radii as large as 40 to 45 microns were carried up to the top of the cloud.

The distribution of air temperature within the cloud as shown in Fig. 1*f* indicates that the lapse rate is about 0.5°C per 100 m, which is very close to the saturated adiabatic lapse rate. The ascending air current was observed throughout the cloud. The velocity of the current was small in the lower part of the cloud, but in the upper part it was found to be about 2 m/sec. Therefore the cloud had the character of upslope fog. According to the author's experience such ascending air currents in stratus cloud are of frequent occurrence on the slope of a mountain. Above the cloud top, however, an air current descending along the slope of Mt. Tokachi predominated on August 10. Both air currents converged along the edge of the cloud and the cloud air mixed with upper dry air.

3. Rotary fog droplet sampler

A fog droplet sampler was constructed for the measurement of droplets in the upper part of fog (Fig. 2). The sampler is principally a circular vertical wheel with a diameter of 35 cm and a width of 4 cm. It is rotated once in 25 minutes by a geared micromotor (Nippon Micromotor Co. Ltd.). The motor is powered by a 7.5 V small dry battery, which was originally employed for the power of the transistor. A belt of celluloid film coated with water-blue dye (OKITA, 1958) is attached to the round side of the wheel. Its length and width are 109 and 4 cm, respectively. The velocity of the displacement of the film, is then 4.35 cm/min. The wheel is enclosed by a thin polyethylene cloth. On the upper side of the apparatus there is a horizontal thin brass plate with area 11 × 37 cm^2 which has in the center a slit with area 1.1 × 4.0 cm^2. The top of the wheel is just under the slit and the spacing between the slit and film is one millimeter or less. The total weight of the sampler is 1.37 kg.

When the wheel is rotated every point of the celluloid film is exposed to the fog air for 15 seconds. It is assumed that the fog droplets fall upon the film with their terminal velocity. This assumption is confirmed when the sampler is kept at constant height (OKITA, 1961). It was found that the measurements were hardly affected by the ascending velocity of the sampler when the velocity was less than 40 cm/sec. This finding can be theoretically examined. The collection efficiency of droplets by a plate 11 cm wide moving vertically through fog with a velocity of 40 cm/sec is calculated by the Langmuir's method (LANGMUIR, 1948). The calculation gives for droplets of 15 and 50 microns radius, the collection efficiency of zero and 0.10 respectively. Therefore the number of small droplets collected on the film by inertial impaction is negligibly small compared with the number of the droplets collected by gravity settling. For droplets with a radius of 50 microns the terminal fall velocity is 26 cm/sec. The equivalent fall velocity by the inertial impaction is $40 \times 0.10 = 4$ cm/sec. Therefore the effect of gravity settling is 6.5 times larger than that of inertial impaction. In other words, the number of large droplets collected when the sampler is ascending is 13 per cent more than when it is kept at constant height.

The sampler was hung at a distance of 10 m below a vinyl balloon. The 3.6 m diameter balloon was tethered by 2 mm diameter nylon cord reinforced by resin. The sampler was operated as follows. First, the time was measured by a stop-watch from the moment when the circuit of the micromotor was closed and the wheel began to rotate. The sampler then ascended with a velocity less than 40 cm/sec. When the sampler reached one of the designated heights, which are usually 50, 100, 150, 200, 250 and 300 m, the time was measured and the sampler was kept at constant height for 30 to 60 seconds; the sampler then ascended to the next designated level. The above operations were repeated several times during the ascent of the sampler.

Since the celluloid film moved at a constant velocity of 4.35 cm/min, the corresponding height of any portion of the film can be determined from the relationship between the height and time. The belt of the film is cut into many small pieces and attached to the glass slides by pressure sensitive cellulose tape. The length of each piece of film is 2 cm, which corresponds to the sampling time about 30 seconds. The counting of the droplets on each piece of film is made by means of a microscope.

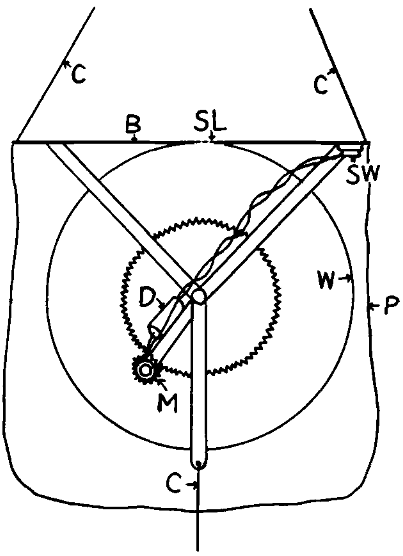

FIG. 2. Rotary fog droplet sampler. W: water-blue coated film; P: polyethylene cloth; M: micromotor; D: dry battery; B: brass plate; C: cord; SL: slit; SW: switch.

If n_{si} is the number of the droplets of radius r_i falling upon 1 cm^2 of the film in one second, the droplet concentration n_i in 1 cm^3 of air is given by $n_i = n_{si}/v_i$ where v_i is the terminal velocity of the droplets. The droplet concentration N and liquid water content W are given by $N = \sum_i n_i$ and $W = \frac{4}{3}\pi\varrho\sum n_i r_i^3$, respectively, where ϱ is the density of water. The concentration of droplets of radii above 3 microns can be obtained satisfactorily by means of the gravity settling method, but the technique is unfavorable for the smaller droplets. Therefore the droplet concentrations shown in the figures of the following chapters do not involve droplets with radii below 3 microns. The measurements by means of an impactor show that such small fog droplets are very few near the ground. However, it is likely that small size droplets are more frequent near the top of deep fogs. Their contribution to the total liquid water content would, on the other hand, be very small.

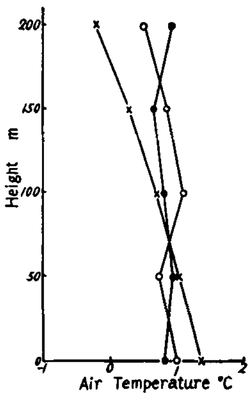

Fig. 3.

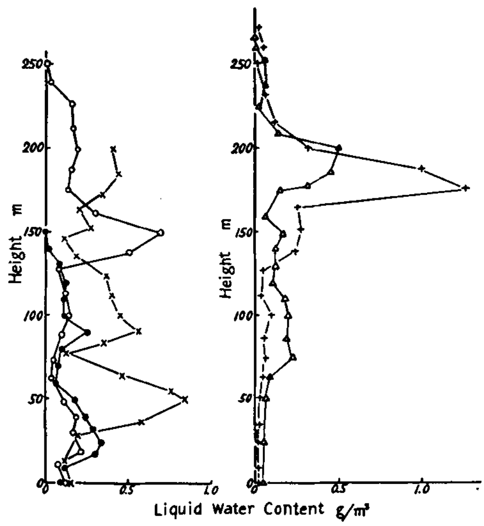

Fig. 4.

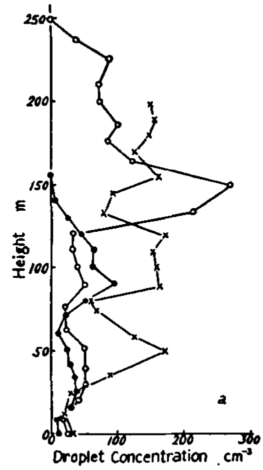

Fig. 5 *a*.

FIG. 3. Temperature profiles on October 18, 1959. ● 0420–0438 JST; × 0535–0546 JST; ○ 0712–0729 JST.

FIG. 4. Vertical distributions of liquid water content on October 18, 1959. ● 18–1, 0352–0417 JST; × 18–2, 0509–0534 JST; ○ 18–3, 0604–0629 JST; + 18–4, 0644–0709 JST; Δ 18–5, 0848–0913 JST.

FIG. 5*a* and *b*. Vertical distributions of droplet concentration on October 18, 1959. For symbols see Fig. 4.

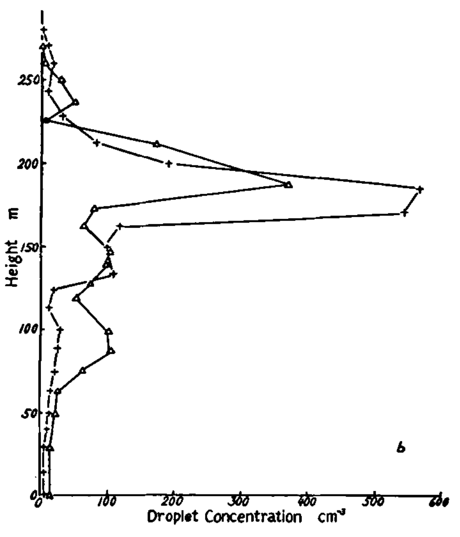

Fig. 5 *b*.

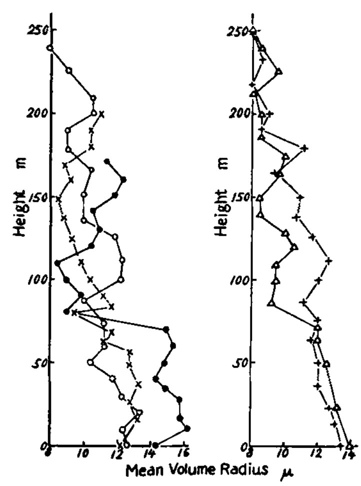

FIG. 6. Vertical distributions of mean volume radius on October 18, 1959. For symbols see Fig. 4.

Therefore the total liquid water content and mean volume radius are assumed to be unaffected by the presence of small droplets. The maximum droplet radius is also measured for each piece of the film.

Between the successive ascents of the sampler the measurements were made of the vertical distribution of air temperature using a thermistor which was hung under the balloon. The observations were made at the ground of the Gakugei University in Asahikawa, Hokkaido, Japan.

4. Observations on October 18, 1959

Stratus cloud occurred at about 0230 JST. The base of the cloud descended to the ground at about 0330 JST. Five droplet samplings were made. The vertical temperature profiles in the fog are shown in Fig. 3. It was found that at about 0430 JST the inversion of temperature still persisted but at about 0540 JST the lapse rate of temperature was superadiabatic throughout the fog layer.

Fig. 4 shows the vertical distributions of liquid water content. In the case of the sample (18–1) the fog top was at about 150 m above the ground and the liquid water was confined to the lowest layer with a maximum content of 0.33 g/m^3 at 25 m. A secondary maximum of 0.25 g/m^3 was found at 90 m. Between 0400 and 0500 JST the fog rapidly developed upward and the liquid water content of the layer above 30 m greatly increased. The maximum content of 0.86 g/m^3 was found at 50 m. The height of the peak liquid water content gradually rose, that is, at 175 m for (18–4) and at 200 m for (18–5). For the samples (18–3) to (18–5) the deep layer of uniform water content existed under the layer of the peak liquid water content.

The top of the fog rapidly rose in its early stage, its height increasing from 150 to 250 m between the samples (18–1) and (18–3), later on, however, the fog did not develop upwards.

The vertical distribution of droplet concentration is shown in Fig. 5. The distribution of the sample (18–1) had a peak value of 96 cm^{-3} at 90 m. The concentration increased rapidly between the samples (18–1) and (18–2) at the level above 30 m. The distribution of (18–2) had peaks of concentration about 160 cm^{-3} at several different heights. But the height of the peaks and the peak concentrations changed rapidly. These rapid changes occurred between successive samples suggesting that the upper part of the fog was in unsteady state. It is surprising to note that, in the upper part of the fog, the droplet concentration always exceeded 100 cm^{-3}. In the later stage the concentration became as large as 570 cm^{-3}, which is comparable with the concentration in cumulus clouds. Although our sampling technique was unfavorable for the measurement of droplets below 3 microns in radius, it is likely that such small droplets were also contained near the top of the fog. The value of mean volume radius at these levels was quite small as shown in Fig. 6; the upper layer then has a structure similar to that of the cumulus clouds which usually have many small droplets. The layer of maximum droplet concentration and minimum mean volume radius is located at 50 to 100 m below the fog top.

In the initial stage of fog (sample (18–1)) the mean volume radius was about 16 microns near the ground; near 100 m it rapidly decreased to about 9 microns. As the fog developed the mean volume radius was reduced to less than 14 microns near the ground and the distribution of the mean volume radius became steady with a maximum value of 14 microns near the base and minimum of 8 microns near the top (see (18–3)).

5. Observations on October 20, 1959

A stratus cloud appeared at about 0300 JST and its base descended to the ground at 0355 JST. Five droplet samplings were made. The fog was dissipating during the last sampling.

The temperature profiles in the fog are shown in Fig. 7. The inversion gradually disappeared and at about 0700 JST the distribution was close to the saturated adiabatic.

Fig. 8 shows the vertical distributions of liquid water content. The fog top was slowly ascending and descending; it was located at 250, above 250, at 190, 250 and 200 m for the samples (20–1), (20–2), (20–3), (20–4) and (20–5), respectively. One of the characteristics of the fog was the vertical uniformity of liquid water content. The mean values of the liquid water content were about 0.1, 0.3, 0.3, 0.25 and 0.2 g/m^3 for the samples (20–1), (20–2), (20–3), (20–4) and (20–5), respectively. Sharp peaks occasionally appeared in individual distributions.

The vertical distributions of droplet concentration are shown in Fig. 9. The figure shows that except for the sample (20–2), the peak concentration above 200 cm^{-3} appeared from 40 to 50 m below the fog top. The presence of numerous small droplets between 40 and 100 m below the fog top is one of the characteristics of the deep fogs on October 18 and 20.

The vertical distributions of mean volume radius are shown in Fig. 10. For the sample (20–1) the mean volume radius gradually decreased with height but for the samples (20–2)

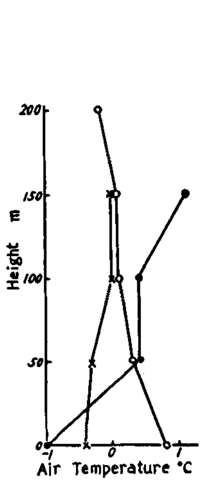

Fig. 7.

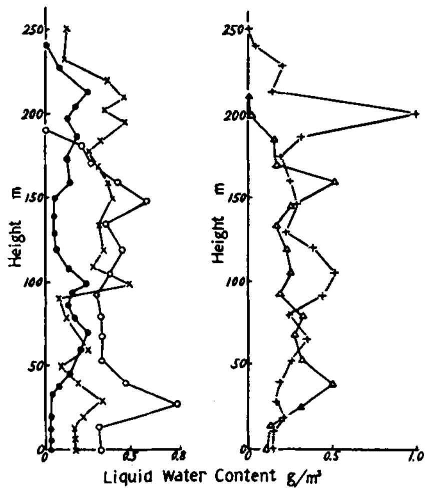

Fig. 8.

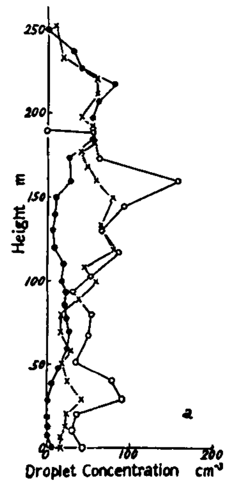

Fig. 9 *a*.

FIG. 7. Temperature profiles on October 20, 1959. ● 0300–0315 JST; × 0444–0500 JST; ○ 0700–0714 JST.

FIG. 8. Vertical distributions of liquid water content on October 20, 1959. ● 20–1, 0410–0435 JST; × 20–2, 0520–0545 JST; ○ 20–3, 0632–0657 JST; + 20–4, 0730–0755 JST; Δ 20–5, 0808–0833 JST.

FIG. 9*a* and *b*. Vertical distributions of droplet concentration on October 20, 1959. For symbols see Fig. 8.

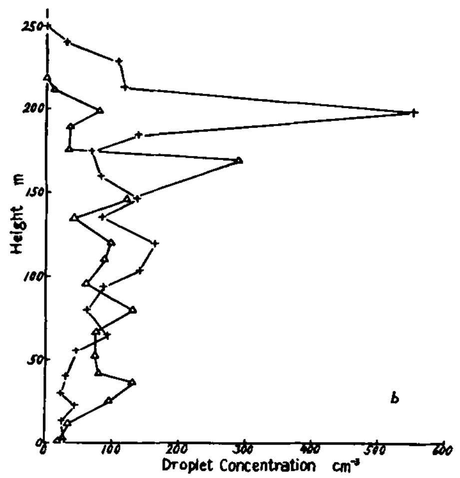

Fig. 9 *b*.

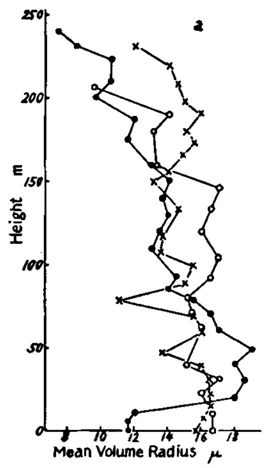

Fig. 10 *a*.

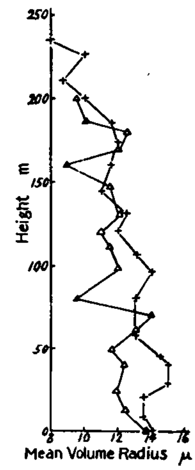

Fig. 10 *b*.

FIG. 10*a* and *b*. Vertical distributions of mean volume radius on October 20, 1959. For symbols see Fig. 8.

to (20–5) its distribution became more uniform throughout the fog layer. Such a change also occurred in the fog of October 18.

6. Observations on October 22, 1959

The fog was formed at about 0300 JST. Five samplings were made. The temperature profiles in the fog are shown in Fig. 11. Before the occurrence of the fog (0235–0247 JST) a large temperature inversion was observed near the ground. After the fog had formed, the inversion was gradually destroyed; between 0500 and 0700 JST an isothermal layer formed in the lower part of the fog while the inversion still remained between 50 m and the top of the fog.

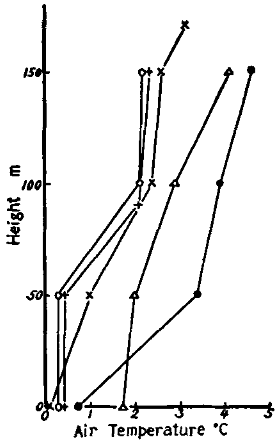

FIG. 11. Temperature profiles on October 22, 1959. ● 0235–0247 JST; × 0417–0436 JST; ○ 0544–0558 JST; + 0651–0705 JST; Δ 0753–0805 JST.

Between 0700 and 0800 JST the air temperature near the ground increased but the air temperature in the upper level also increased, so that the temperature inversion still continued.

Fig. 12 shows the vertical distributions of liquid water content. During the sampling (22–1) the fog was forming and four samplings were made successively at intervals of about 6 minutes. In the early stage of the fog formation, the peak liquid water content was found near the ground. The level of the peak then rose to 16 m at the second and third samplings, and to 22 m at the fourth sampling. Between the third and fourth samplings the liquid water content increased throughout the fog layer. The peak content was located at a constant level of about 20 m. The top of the fog rose to 50 m at (22–2) and to 100 m at (22–3); it remained at about 100 m until 0620 JST; and then began to descend.

Figs. 13 and 14 show the vertical distributions of droplet concentration and mean volume radius, respectively. Fig. 13*a* indicates that the droplet concentration slowly increased in the early stage of fog formation and that the droplet concentration was always below 40 cm^{-3}. The mean volume radius had increased to above 11.5 microns when the first sampling was made.

The layer just below the fog top frequently contained small droplets as indicated by the samples (22–2), (22–3) and (22–4) in Fig. 14*b*. The shape of the profiles of both droplet concentration and mean volume radius varied from sample to sample. In no samples the droplet concentration exceeded 100 cm^{-3}.

7. Observations on October 29, 1959

A ground fog appeared and rapidly developed at about 0310 JST. Three droplet samplings were made. The temperature profiles in the fog are shown in Fig. 15. The figure indicates that the temperature inversion continued even in the fog layer except in the dissipating stage of the fog.

The profiles of liquid water content are shown in Fig. 16. The fog top was located at about 100, 120 and 75 m for the samples (29–1), (29–2) and (29–3), respectively. The profiles of liquid water content had their peak at about 50 m. Although the fogs on October 22 and 29 had nearly the same thickness, the liquid water content on October 29 was usually much larger than that on October 22, with the maximum value as high as 1.6 g/m^3. The profiles of droplet concentration shown in Fig. 17 indicate that in the middle layer of the fog the droplet concentration sometimes exceed 100 cm^{-3}. The profiles of mean volume radius shown in Fig. 18 indicate that small droplets predominate at the top of the fog. Comparing the values of mean volume radius in Figs. 14 and 18 with those in Figs. 6 and 10 it seems that the droplet size is independent of the thickness of fog.

8. Summary of part I

The vertical structures of four radiation fogs and one stratus cloud are presented in the preceding sections. The data for October 18, 20 and for October 22, 29 are examples of deep and shallow radiation fogs, respectively.

It has been thought that fogs and stratus clouds formed by slow cooling process have a larger droplet size and smaller droplet concentration than the clouds formed by adiabatic cooling. However, the droplet observations of fog and stratus cloud have been made mainly near their base. The observations described in the preceding chapters indicate that the upper part of a deep radiation fog or stratus cloud has the same physical structure as the cumulus clouds, that is, there are many small droplets, with a concentration above 100 cm^{-3}. Small droplets are also present near the top of shallow fog.

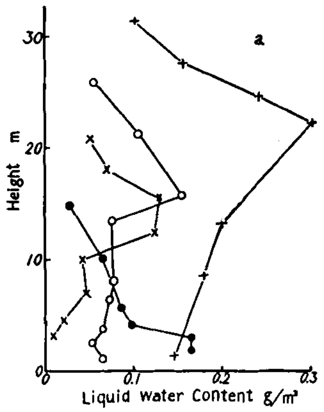

Fig. 12 *a*.

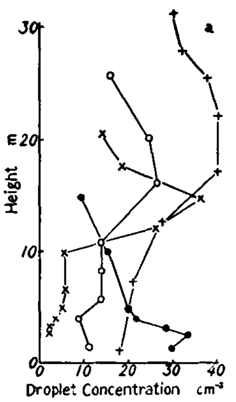

Fig. 13 *a*.

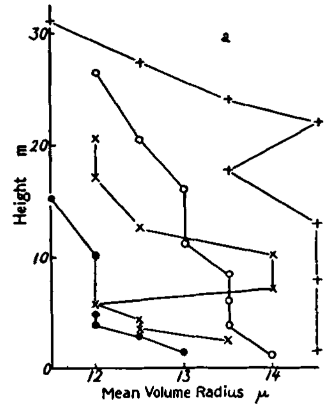

Fig. 14 *a*.

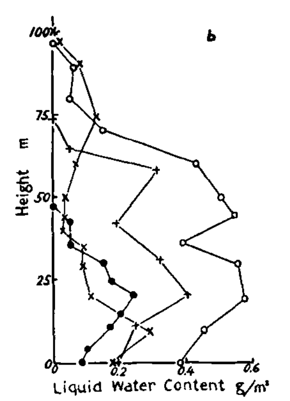

Fig. 12 *b*.

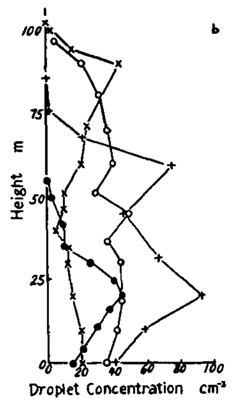

Fig. 13 *b*.

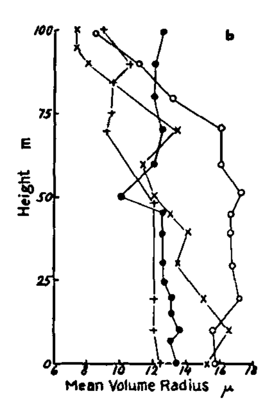

Fig. 14 *b*.

FIG. 12. Vertical distributions of liquid water content on October 22, 1959. (*a*) Sample 22–1, 0305–0330 JST: ● first sampling; × second sampling; ○ third sampling; + fourth sampling. (*b*) ● 22–2, 0348–0413 JST; × 22–3, 0502–0527 JST; ○ 22–4, 0606–0629 JST; + 22–5, 0711–0736 JST.

FIG. 13. Vertical distributions of droplet concentration on October 22, 1959. (*a*) For symbols see Fig. 12*a*. (*b*) For symbols see Fig. 12*b*.

FIG. 14. Vertical distributions of mean volume radius on October 22, 1959. (*a*) For symbols see Fig. 12*a*. (*b*) For symbols see Fig. 12*b*.

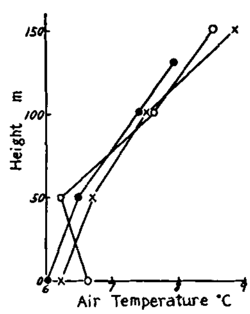

FIG. 15. Temperature profiles on October 29, 1959. ● 0437–0450 JST; × 0600–0609 JST; ○ 0657–710 JST.

In the summers of 1944 to 1945 the droplet samples in the upper part of sea fog were obtained by manned captive balloon observations at Nemuro. The examples of the vertical distributions of the droplet concentration and liquid water content of sea fog are shown in Fig. 19 (HANAJIMA, 1945 and OGUCHI, 1949), which also indicates that in the upper part of the sea fog the droplet concentration is above 100 cm^{-3}. It is unlikely that the present condensation theory of fog formation can explain these observational results and further information of the mechanism of droplet formation especially in its dynamic aspects are needed.

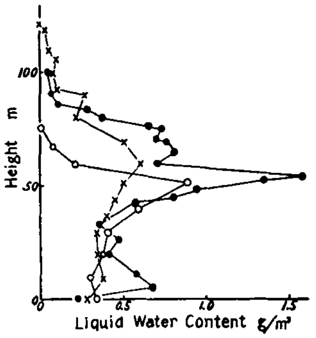

Fig. 16.

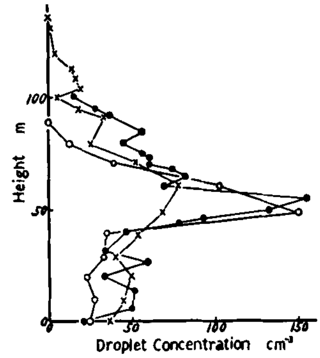

Fig. 17.

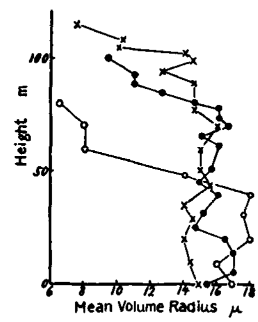

Fig. 18.

FIG. 16. Vertical distributions of liquid water content on October 29, 1959. ● 29–1, 0359–0424 JST; × 29–2, 0527–0552 JST; ○ 29–3, 0625–0650 JST.

FIG. 17. Vertical distributions of droplet concentration on October 29, 1959. For symbols see Fig. 16.

FIG. 18. Vertical distributions of mean volume radius on October 29, 1959. For symbols see Fig. 16.

9. Mechanism of formation and growth of ordinary fog droplets

The mechanism of formation and growth of ordinary cloud and fog droplets is one of the important problems in cloud physics. In the winter of 1930 to 1931 FINDEISEN (1932) measured, by means of the corona method, the size distributions of the droplets in radiation fog and in the fog artificially produced in a small room. Analysing the results of the measurements in the artificial fog he concluded that the growth of the fog droplets was caused by the mutual coalescence of the droplets due to the difference of the velocity of fall between large and small droplets. He further supposed that the same phenomena would also occur in natural fog. SCHUMANN (1940) also mentioned that the mutual coalescence is the most important agent for the growth of the fog droplets. However, according to the calculations of HOWELL (1949), KRAUS & SMITH (1949), MORDY (1959) and others, the droplet size distribution can be explained only by the process of condensation.

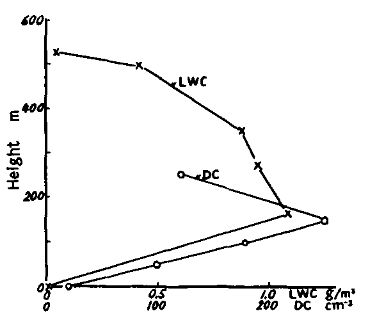

FIG. 19. Vertical distributions of liquid water content and droplet concentration of sea fog. LWC: liquid water content; DC: droplet concentration.

As described in section 6, the droplet sampling was made during the formation of fog on October 22. The observation shows that within ten minutes after the occurrence of the fog the mean volume radius rapidly increased to above 11.5 microns and afterwards varied only gradually.

According to Mordy's calculation the cloud droplets formed by condensation in the air rising with a velocity of 15 cm/sec (which corresponds to the cooling rate of 1.65°C/hr) have a mean linear radius of about 8 microns at five minutes after the formation of the cloud; the mean linear radius then increases more slowly

The relationship between mean linear radius and mean volume radius of radiation fog droplets obtained by the author and shown in Fig. 20, indicates that the mean linear radius of 8 microns corresponds to the mean volume radius of 11.5 microns. The rate of temperature fall at the time of occurrence of fog is usually about 1 to 1.5°C/hr as shown in Figs. 3, 7, 11 and 15. Therefore the measured growth rate of small droplets in the initial stage of fog formation is in good agreement with the results of Mordy's calculation.

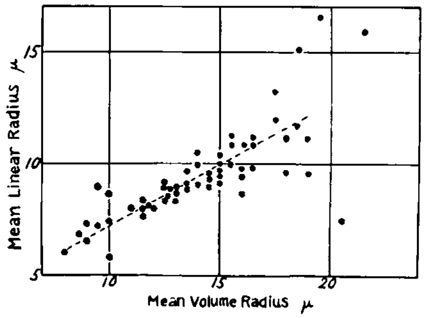

Fig. 20. Relationship of mean linear radius versus mean volume radius of radiation fog droplets.

The observation further indicates that the droplet concentration is only 1 to 40 per cm^3 which is too small for coalescence between droplets to occur. It is further observed that the droplet concentration does not decrease but increases within 30 minutes after the formation of the fog. Therefore it may be concluded that the condensation is the main agent for the growth of ordinary droplets in the fog.

Part II. Vertical change of large droplet size in radiation fog and stratus cloud

10. The analysis of the data of radiation fog in 1959

As the mechanism of the formation of large droplets in fog and stratus cloud is one of the important subjects in cloud physics, the results of the observation of large droplets will be described in more detail.

Some of the plots of maximum droplet radius against height in radiation fog are shown in Fig. 21. From the figure it is evident that in most cases when large droplets (with radii above 50 microns, say are observed on the ground in deep fogs, large droplets are also found in the upper layer of the fog (for example, samples (18–3), (20–4) and (20–5)). The samples (18–2) and (18–4) are examples in which there are no such large droplets throughout the fog layer.

As shown in Fig. 1 summer stratus cloud also contains near the top large droplets with radii about 45 microns. Takahashi (1952) found large droplets with a radius of about 165 microns just below the top of precipitating sea fog. Therefore, it may be concluded that the presence of large droplets near the top is a necessary condition for the production of drizzle in the deep fog and stratus cloud.

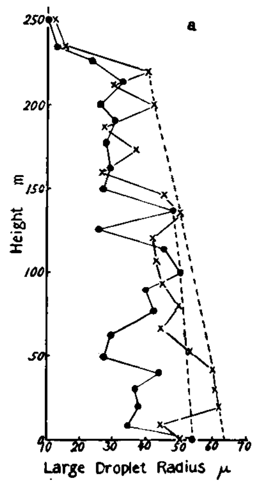

Fig. 21 *a*.

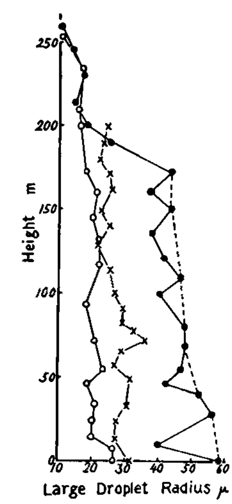

Fig. 21 *b*.

Fig. 21. Relationship of maximum droplet radius versus height in radiation fog of 1959. (*a*) ● 18–3; × 20–4. (*b*) × 18–2; ○ 18–4; ● 20–5.

In this and the following sections the rate of growth by accretion of large droplets falling through deep fog or stratus cloud layer, will be discussed.

The plots of the maximum droplet radius against height as shown in Fig. 21 have irregular form, but it is seen that the maximum radius decreases with increasing height. Although it is difficult to accurately obtain the growth rate of large droplets from these plots, we tentatively draw a line connecting the peaks in the plots (see broken lines in the figure) and regard the lines as representing the growth of the largest droplets in the fog. For example, in the case of the sample (18–3) it is considered that the droplet with a radius of 47 microns at 136 m grows to a droplet of 54 microns in radius near the ground. It then follows that the increment ΔR_m of the radius of droplet during its fall is $\Delta R_m = 54–47 = 7$ microns.

If it is assumed that there is no vertical air current and that the growth of large droplets by condensation is negligible compared with the growth by coalescence with smaller droplets, the increase of the radius of a large droplet dR during its fall for a distance dz is given by the equation

$$dR = \frac{W}{4}\left(\frac{R+r}{R}\right)^2\left(\frac{v_l - v_s}{v_l}\right)Edz, \qquad (1)$$

where r is the radius of a small droplet, v_l and v_s the terminal velocity of the large and the small droplets, respectively, W is the liquid water content and E is the collection efficiency between the large and the small droplets. Therefore if the parameters on the right-hand side of the equation are known dR can be calculated. The assumptions will be valid in the mature stage of deep fog, where the mean volume radius is nearly constant with time.

The values of W and r for which the mean volume radius is taken are obtained from Figs. 4, 6, 8 and 10. The collection efficiency E is calculated by Langmuir's method. The

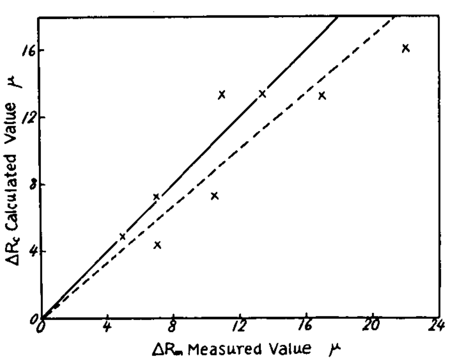

FIG. 22. Comparison of measured and calculated ΔR.

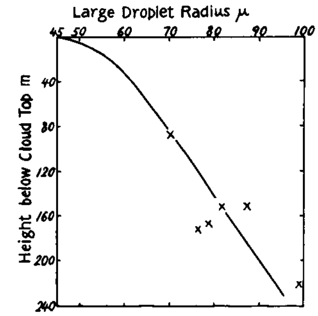

FIG. 23. Growth of large droplets in stratus cloud on August 10, 1959.

measured value of the radius of a large droplet at height 130 to 210 m is taken as the initial droplet radius. The evaluation of dR is made for the successive 50 m intervals on the assumption that the liquid water content W and mean volume radius r are constant in each interval. The total increase ΔR_c is the summation of dR. The plots of ΔR_c against ΔR_m shown in Fig. 22 scatter widely. But, on the average, the measured value is about 20 per cent larger than the calculated one.

11. The analysis of the data of stratus cloud on August 10, 1959

The ascending air currents were observed in the stratus cloud over the mountain slope as described in chapter 2. The wind velocity measured on the slope of Mt. Tokachi on August 10, 1959 was 2 m/sec. The mean gradient of the slope is about 0.13, so that the vertical component of wind velocity is calculated to be 26 cm/sec.

When the ascending air current with velocity V exists in the stratus cloud the increase of the radius of large droplets falling through the cloud is given by the equation

$$dR = \frac{W}{4}\left(\frac{R+r}{R}\right)^2\left(\frac{v_l - v_s}{v_l - V}\right)Edz. \qquad (2)$$

We shall apply equation (2) to the droplet growth in the stratus cloud on August 10, 1959.

First, it is assumed that the droplets grow to a 45-micron radius while ascending to the top of the cloud before their descent. It is then reasonable to assume that V is equal to 24 cm/sec, which is the terminal velocity of 45-

micron radius droplets. The measurements show that the mean liquid water content and mean volume radius are 0.4 g/m^3 and 11 microns, respectively. These values are chosen as the values of W and r in equation (2). The relation between R and z can then be calculated.

Fig. 23 shows the result of the calculation. The relationships between droplet radius and height obtained from Fig. 1 are also plotted in the figure. Good agreement between the calculated and measured values is seen.

12. Discussion

Fig. 23 suggests that the collection efficiency obtained by Langmuir's method gives correct values. On the other hand, Fig. 22 shows that the increase of droplet radius ΔR_c in radiation fog calculated using Langmuir's method gives values 20 per cent smaller than those measured. It is difficult to account for the discrepancy of the two measurements. One possible explanation is that the vertical air currents exist also in the deep fog, so that the growth time of large droplets increases. The presence of large droplets near the fog top described in section 10 suggests the presence of such ascending air current.

In the later stage of the deep radiation fog the saturation adiabatic lapse rate of air temperature is established as demonstrated theoretically and observationally by FLEAGLE and others (1953). Our measurements of temperature profile described in the preceding chapters also confirm this phenomenon. In this case it is probable that if the lapse rate in the fog exceeds the saturated adiabatic lapse rate vertical air motion will set in.

In conclusion, although our observations confirm that Langmuir's theory is valid for the growth of large droplets in fog and stratus cloud at least for the first approximation, further study of the precipitation mechanism in fog and stratus cloud in its dynamical aspects is needed in order to clarify the phenomena in more detail.

Recently KINZER & COBB (1958) made laboratory measurements of the collection efficiency between large and small droplets. According to them the collection efficiency E' is given by

$$E' = (dm/dt)/\pi R^2 W v_l, \qquad (3)$$

where dm/dt is the rate of increase of large droplet mass, other symbols being the same as in equation (1). According to Langmuir the collection efficiency E is given by

$$E = (dm/dt)/\pi(R+r)^2 W(v_l - v_s). \qquad (4)$$

If the difference of radius between large and small droplets is large, both collection efficiencies become identical. However, when the difference is small these definitions give different results.

According to the measurements of Kinzer and Cobb the values of E and E' are nearly the same for large droplet with a radius of about 45 microns and for mean volume radius of small droplets about 9.3 microns. If the values of E and E' are the same equations (3) and (4) give considerably different values of dm/dt. For example, if we assign 45 and 12 microns for the values of R and r, respectively, the Langmuir's method gives for dm/dt a value 36 per cent larger than the measured value of Kinzer and Cobb. Although our observations seem to confirm the validity of Langmuir's theory for the range of droplets with a radius of 34 to 85 microns, more exact observations are required to explain the difference of Langmuir's theory and Kinzer and Cobb's measurements.

REFERENCES

FINDEISEN, W., 1932, Messungen der Grösse und Anzahl der Nebeltropfen zum Studium der Koagulation inhomogenen Nebels, *Beitr. Geophys.*, **35**, p. 295

FLEAGLE, R. G., PARROTT, W. H., and BARAD, M. L., 1953, Theory and effects of vertical temperature distribution in turbid air. *Journ. Met.*, **9**, p. 53.

HANAJIMA, M., 1945, Measurements of total water content and liquid water content in fog. *Study of Fog in Chishima and Hokkaido*, No. **26** (in Japanese).

HOWELL, W. E., 1949, The growth of cloud drops in uniformly cooled air. *Journ. Met.*, **6**, p. 134.

KINZER, G. D., and COBB, W. E., 1958, Laboratory measurements and analysis of the growth and collection efficiency of cloud droplets. *Journ. Met.*, **15**, p. 138.

KRAUS, E. B., and SMITH, S., 1949, Theoretical aspects of cloud drop distributions. *Australian Journ. Sci. Res.*, **2**, p. 376.

LANGMUIR, I., 1948, The production of rain by a chain reaction in cumulus clouds of temperatures above freezing. *Journ. Met.*, **5**, p. 175.

MORDY, W., 1959, Computations of the growth by condensation of a population of cloud droplets. *Tellus*, **11**, p. 16.

OGUCHI, H., 1949, On the method of the measurement of the size and number of fog droplets. *Low Temperature Science*, **2**, p. 105 (in Japanese).

OKITA, T., 1958, Water-blue film method for measurement of cloud and fog droplets. *Journ. Met. Soc. Japan*, **31**, p. 237.

OKITA, T., 1961, Size distribution of large droplets in precipitating clouds. *Tellus*, **13**, p. 509.

SCHUMANN, T. E. W., 1940, Theoretical aspects of the size distribution of fog particles. *Quart. Journ. Roy. Met. Soc.*, **66**, p. 195.

TAKAHASHI, Y., 1952, Sea fog of advection type over Oyashio. *Seventh Pacific Science Congress*, **3**, p. 1.